Sensors & Transducers, Vol. 196, Issue 1, January 2016, pp. 75-81

Sensors & Transducers

http://www.sensorsportal.com

An Automatic Segmentation Method for Printed Circuit Board Welding Component under Stereo Optical Microscope

[1] Yi LIU, [1] Mei YU, [1] Li CUI, [1] Gang-Yi JIANG, [1, 2] Yi-Gang WANG and [1, 2] Sheng-Li FAN

[1] Faculty of Information Science and Engineering, Ningbo University, Ningbo 315211, China
[2] Department of Information, Ningbo Institute of Technology, Zhejiang University, Ningbo 315010, China
[1] Tel.: 13857476528, fax: 0574-87608138
E-mail: jianggangyi@126.com

Received: 28 June 2014 /Accepted: 18 August 2014 /Published: 31 January 2016

Abstract: Common image segmentation methods only consider the single image and cannot extract welded components automatically and exactly. GrabCut algorithm need draw a rectangle which labels possible foreground region and determines general location to segment desired object. In this paper, a novel automatic GrabCut algorithm is proposed for segmenting Printed Circuit Board (PCB) welding component under stereo optical microscope. The proposed method considers the characteristic of welded component on the foreground region of PCB and uses unparallel stereo microscopic image to obtain foreground mask of disparity map. To obtain parallel stereo microscopic image, Quasi-Euclidean epipolar rectification algorithm is utilized into original unparallel stereo microscopic image. Then, disparity map is obtained by using the non-local filter algorithm on parallel stereo microscopic image, and foreground mask of disparity map is extracted by applying the mean-threshold method. Finally, rectified microscopic image is segmented by initializing GrabCut's trimap *T* with foreground mask of disparity map. The experimental results show that the proposed method can extract PCB welding component automatically and accurately without user intervention and is much better than adaptive binary method. *Copyright © 2016 IFSA Publishing, S. L.*

Keywords: Image segmentation, Stereo microscopic image, Printed Circuit Board welding component, Foreground mask of disparity map, Automatic GrabCut.

1. Introduction

Intelligent detection and location analysis of Printed Circuit Board (PCB) welding components need to extract accurately PCB image's external features [1-2], such as welding condition, wiring condition, and positioning hole. Therefore, the PCB image must be processed high efficiently. As we know, image segmentation is a process of dividing an image into several characteristic regions, and plays a virtual role in detection and location of PCB welding components.

In recent years, many researches on image segmentation have been reported [3-4], such as threshold methods [5], region-based methods [6], edge detection methods [7], clustering methods [8], superpixel based methods [9], graph-based methods [10], and other hybrid methods [11]. Threshold

segmentation methods are widely used on account of their simplicity and efficiency. Hammouche K. proposed a multilevel thresholding method to determine the number of thresholds and the adequate threshold for a fast image segmentation [12]. However, conventional histogram-based threshold algorithms can only separate those areas which have obvious different gray levels. Moreover, they cannot perform well for images whose histograms are nearly unimodal. For edge detection methods, the most commonly applied edge detection operators include Canny, Sobel, Prewitt and Laplacian. They mainly focus on those pixels which locate on the boundaries of object [13]. Therefore, it is hard to yield closed contours and homogeneous regions. While region growing, splitting, merging and other region-based methods often deal with spatial repartition of image feature information to obtain closed and homogeneous regions. Geometric flows are inherently good at controlling geometric shape evolution. A geometric flow-based formulation and solution for image segmentation is proposed by Ye J. [13]. However, over-segmentation and under-segmentation are critical difficulties to be considered in those methods. Clustering methods can generate better segmentation effects with the consideration of viewing image as tremendous multidimensional data and classifying an image into different portions according to certain homogeneous criterion. Wang proposed an adaptive spatial information-theoretic fuzzy clustering algorithm to improve the robustness of the conventional fuzzy c-means clustering algorithms for image segmentation [15]. But over-segmentation is the problem that must be solved and feature extraction is also an important factor for clustering. Superpixel can provide meaningful grouping cues to guide segmentation and reduce the computational complexity. Yang introduces a novel 3-D geometry enhanced superpixels for RGB-D data [16]. But sometime the segmentation performance depends on the superpixel generation approach. Graph-based image segmentation methods are modeled to divide a graph into several sub-graphs such that each of them represents a meaningful object in the image, but they always need user intervention [17-18]. In conclusion, though much emphasis has been put on image segmentation and many methods have been proposed in recent decades, there is neither universal segmentation approach for all kinds of images nor an automatic and effective segmentation approach for PCB welding component under digital stereo optical microscope.

Common image segmentation methods only take consider of single image but they do not use the useful information offered by stereo image. Obviously, the location and appearance of the desired object is difficult to acquire. Consequently, welded components are hard to be segmented availably in the real complex PCB scenery. GrabCut algorithm [17] cannot extract desired object automatically. But it can segment the object effectually with manually drawing a rectangle. Generally, PCB welding components locate at the foreground region of disparity map.

Considering the reasons of above, the proposed method uses unparallel stereo microscopic image to obtain foreground mask of disparity map for determining the general position of PCB welding component and initialing the trimap T of GrabCut to segment PCB welding component without any user intervention.

2. Proposed Automatic GrabCut Method for PCB Welding Component Segmentation

In this paper, an attempt to obtain a solution to realize automatic PCB welding component segmentation is done. Firstly, the proposed automatic GrabCut (A-GrabCut) method rectifies original captured stereo microscopic image to parallel stereo microscopic image by employing the Quasi-Euclidean epipolar rectification algorithm. Secondly, to obtain disparity map of microscopic image, the non-local filter algorithm is utilized into rectified stereo microscopic image. Then, foreground mask is extracted from disparity map by using the mean-threshold method. Finally, extracted foreground mask initializes the trimap T of GrabCut algorithm, and automatic segmentation for PCB welding component starts on rectified stereo microscopic image. The whole procedure of proposed A-GrabCut method for PCB welding component segmentation of stereo microscopic image is illustrated as Fig. 1, which will be described in detail in the following subsections.

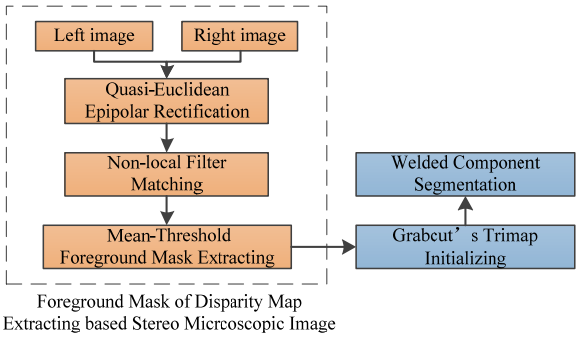

Fig. 1. Procedure of A-GrabCut method for PCB welding component segmentation.

2.1. Quasi-Euclidean Epipolar Rectification

There are errors between inside equipment setup of real microscope and ideal parallel stereo microscopic system. And small bias of parallel optical path leads to large offset of micro amplification imaging. Therefore, the same 3D point does not locate identical vertical coordinate in stereo microscopic image. It is very important to rectify

epipolar for requirement of parallel stereo microscopic image.

Because of the limitation of microscope's depth of focus, the camera calibration of stereo optical microscopic system is tedious and difficult. The method that rectifies stereo microscopic image by utilizing camera's internal and external parameters is not suitable for stereo optical microscopic system. However, the desired homograph matrixes of unrectified stereo microscopic image can be obtained by using Quasi-Euclidean epipolar rectification method [19], which find matching points of stereo microscopic image to make rectified error E approach 0. The formula can be expressed as follows:

$$E(x_l, y_l, x_r, y_r) = X_l^T H_l^T [e_1]_\times H_r X_r = 0, \quad (1)$$

where (x_l,y_l) and (x_r,y_r) are the matching points of the left and right views of the original stereo microscopic image, and X_l and X_r are homogeneous coordinates of (x_l,y_l) and (x_r,y_r). $\boldsymbol{H_l}$ and $\boldsymbol{H_r}$ are corresponding homograph matrix of the left and right views of the original stereo microscopic image for epipolar rectification. $\boldsymbol{[e_1]_\times}$ is antisymmetric matrix of unit direction vector $e_1 = (1,0,0)$.

Finally, rectified left and right microscopic images I_l^{rec} and I_r^{rec} can be computed as follows:

$$\begin{cases} I_l^{rec} = H_l I_l^{org} \\ I_r^{rec} = H_r I_r^{org} \end{cases}, \quad (2)$$

where I_l^{org} and I_r^{org} are the left and right views of the original stereo microscopic image respectively.

Quasi-Euclidean epipolar rectification algorithm can work well without calibrating camera's internal and external parameters under stereo optical microscopic system. Therefore, it meets the requirement of stereo optical microscopic system's epipolar rectification and reduces the difficulty of stereo microscopic image epipolar rectification.

2.2. Foreground Mask Generation

This section mainly includes that disparity map of microscopic image is solved by the non-local filter method and foreground mask is obtained from disparity map by using proposed mean-threshold method.

2.2.1. Non-local Filter Matching

The original stereo microscopic image has been rectified by section (2.1). To obtain disparity map of microscopic image, stereo matching is need to apply to parallel stereo microscopic image I_l^{rec} and I_r^{rec} .Unlike common traditional approaches which build similar function based on local window or irregular shape, the non-local filter approach [20] connects all image pixels by using minimum spanning tree (MST) on which all weight sum is the most lowest.

$$S(p,q) = S(q,p) = \exp(-\frac{D(p,q)}{\sigma}) \quad (3)$$

is the similarity between node p and q in the MST, where σ is a constant used to adjust the similarity between two nodes. $D(p,q)=D(q,p)$ is the distance between node p and q.

The joint bilateral filter [21] can then be directly extended to MST structure:

$$\begin{aligned} C_d^A(p) &= \sum_q S(p,q) C_d(q) \\ &= \sum_q \exp(-\frac{D(p,q)}{\sigma}) C_d(q) \end{aligned}, \quad (4)$$

where $C_d(q)$ is the matching cost for pixel p at disparity level d, and $C_d^A(p)$ is the aggregated cost. Aggregation using MST relaxes two ambiguities to a single ambiguity σ .

Two nodes' distance can be accumulated from leaf nodes tracking to root node in the MST. The formula can be expressed as follows:

$$\begin{aligned} C_d^A(v) &= S(P(v),v) \cdot C_d^A(P(v)) \\ &+ [1 - S^2(v,P(v))] \cdot C_d^{A\uparrow}(P(v)) \end{aligned}, \quad (5)$$

where v is the node in the MST, and $P(v)$ is the parent node of v. $C_d^{A\uparrow}(P(v))$ is the accumulated aggregation cost from leaf nodes to node $P(v)$. Consequently, its computation complex is very low and only requires a total of 2 addition/subtraction operations and 3 multiplication operations. This paper just considers the disparity map of the left microscopic image $I_l^{dm}(i,j)$.

2.2.2. Mean-threshold Foreground Mask Extracting

Supposed that PCB surface and camera's image plane are parallel, the disparity of same plane should be identical. Generally, it is a plane for PCB welding components, such as chips and resistances. The result is indeed after experimental verification. Obviously, the large disparity region that is foreground region is required to be extracted typically. And the proportion of those regions is large in microscopic image.

For this purpose, the histogram can be calculated from disparity map of microscopic image I_l^{disp} . And the probability of histogram can be formulated as follows:

$$P(k) = n_k / N \ , \quad (6)$$

where N is the total number of an image pixels, and n_k is the number of pixel at disparity level k. $P(k)$ is the probability of occurrence at disparity level k.

Generally, mismatch and noise exist in disparity map of microscopic image. To reduce the influence of mismatch and noise of which the proportion is small in disparity map, the mean of disparities is solved by selecting fore M proportion of sorted n_k. The formula can be expressed as follows:

$$mean = \frac{1}{M} \sum_{i=1}^{M} r_i \quad (7)$$

Finally, foreground mask of disparity map is obtained by selecting the disparity above mean disparity:

$$I_l^{fm}(i,j) = \begin{cases} 255, & if \quad I_l^{dm}(i,j) > mean \\ 0, & else \end{cases}, \quad (8)$$

where $I_l^{dm}(i,j)$ is the disparity of coordinate (i,j) in disparity map of left microscopic image, and $I_l^{fm}(i,j)$ is the disparity of coordinate (i,j) in foreground mask image of left disparity map.

2.2.3. GrabCut Algorithm and PCB Welding Component Segmentation

GrabCut algorithm based on Gussian Mixture Model (GMM) is an image segmentation method realized by combining with graph cut. The GrabCut technique considers the array $z=(z_1,\ldots,z_n,\ldots,z_N)$ of N pixels in an image where $z_i=(R_i, G_i, B_i)$, $i \in [1,...,N]$. The segmentation is defined as an array $a = (a_1,\ldots,a_i,\ldots,a_N)$, $a_i \in \{0,1\}$ and assigns a label to each pixel of the image, indicating whether it belongs to the foreground or the background. A trimap T is given by the user, which consists of three regions: *TF*, *TB* and *TU*, each one including initial background, foreground, and uncertain pixels respectively. Pixels belonging to *TF* and *TB* are considered as foreground and background respectively, whereas those belonging to *TU* are labeled through by the algorithm.

A full covariance GMM of K components of foreground and background pixels is parameterized as follows:

$$\underline{\theta} = \{\pi(a,k), \mu(a,k), \Sigma(a,k), a = \{0,1\}, k = 1...K\}, \quad (9)$$

where π , μ , Σ respectively represent the weight, mean vector, covariance matrix of the GMM.

The energy function for segmentation of GrabCut technique is

$$E(\underline{\alpha}, k, \underline{\theta}, z) = U(\underline{\alpha}, k, \underline{\theta}, z) + V(\underline{\alpha}, z), \quad (10)$$

which consists of a region term U and edge term V. The region term U based on Gaussian probability distributions $p(\cdot)$ and mixture weighting coefficients $\pi(\cdot)$ computes the likelihood of a pixel to belong to certain label. The formula is expressed as follows:

$$U(\underline{\alpha}, k, \underline{\theta}, z) = \sum -\log p(z_i | a_i k_i, \underline{\theta}) - \log \pi(a_i, k_i) \quad (11)$$

Edge term V reflects the penalty of discontinuity between neighborhood pixel m and n.

The main problem of original GrabCut technique is need to draw a rectangle by user to initialize the trimap T for computing the initial GMM. The proposed method locates welded component general position automatically to compute the initial GMM. The results of trimap T by using $I_l^{fm}(i,j)$ *are:* $TU = \{z_i \in mask\}$, $TB = \{z_i \notin mask\}$, where mask is the region consisted of pixel value that is 255 of $I_l^{fm}(i,j)$. According to the lowest energy principle and the initialized trimap T, the final segmentation is generated by graph cut, which is based on Min-Cut/Max-Flow algorithm [22].

3. Experiment and Discussion

In order to verify the proposed method sufficiently, a lot of experiments are conducted. Stereo optical microscope stage is used to capture stereo microscopic image. As shown in Fig. 2, the test stage includes a type of ZOOM460N stereo optical microscopic, which made in Nanjing Wavelength Opto-Electronic Technology Co., Ltd. The bottom is objective table on which a PCB is placed. Common objective transmits information of each to two top eyepieces via two optical paths. The system's eyepieces are connected directly to two types of 902B camera produced by WATEC Company from Japan. And the size of 704×576 per frame is sampled by USB. The test environment: OPENCV2.4.8 and VS2012 in PC (Intel Core(TM) i3 CPU 3.19 GHz, 1.74G memory).

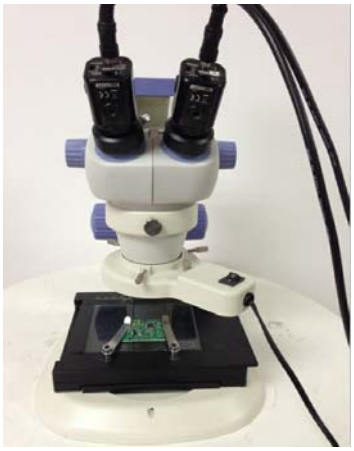

Fig. 2. Digital stereo optical microscope.

In this paper, original stereo microscopic image used in the experiment is shown in Fig. 3. And stereo microscopic image after epipolar rectification is shown in Fig. 4.

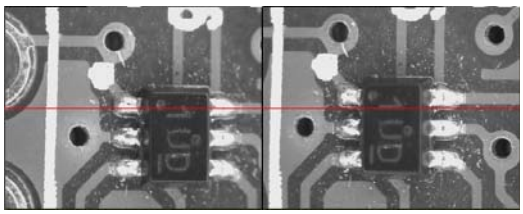

Fig. 3. Original stereo microscopic image.

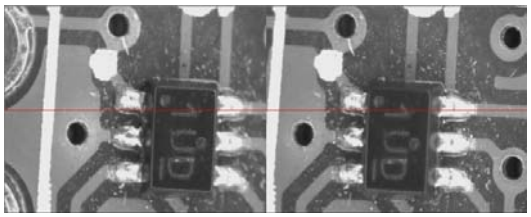

Fig. 4. Rectified stereo microscopic image.

The left disparity map obtained by matching method is shown in Fig. 5 (a). The foreground mask image of left disparity map is shown in Fig. 5 (b). Proportion parameter M is 0.8 in this paper.

(a) (b)

Fig. 5. (a) Left disparity map; (b) Foreground mask image of left disparity map.

3.1. Comparison with User Intervention Segmentation

In the first contrast experiment, the intention is to compare the segmentation effects between the proposed A-GrabCut method and common user intervention segmentation method. There have two realized user intervention segmentation methods in OPENCV's samples. Therefore, our contrast experiment is between the proposed A-GrabCut method and watershed method [23] and original GrabCut method. The main difference between two user intervention methods is that watershed method selects two kinds of elements with user's mouse at any position of image but original GrabCut method only need draw a rectangle.

Fig. 6 shows the manual marks and segmentation effects of user intervention segmentation methods and the visual effect of proposed A-GrabCut method. As shown in Fig. 6 (b), Fig. 6 (d) and Fig. 6 (f), the desired foreground object is segmented efficiently from complex background by three methods. However, proposed A-GrabCut method can generate satisfied result automatically without any manual marks on image in Fig. 6 (e) and Fig. 6 (f). Moreover, watershed method and original GrabCut method need mark image correctly in Fig. 6 (a) and Fig. 6 (c), and original GrabCut method requires many iterative computations to obtain final segmentation if the mark is non-ideal.

So in brief, the proposed A-GrabCut method can obtain the same good segmentation result as two common user intervention segmentation methods without any user intervention.

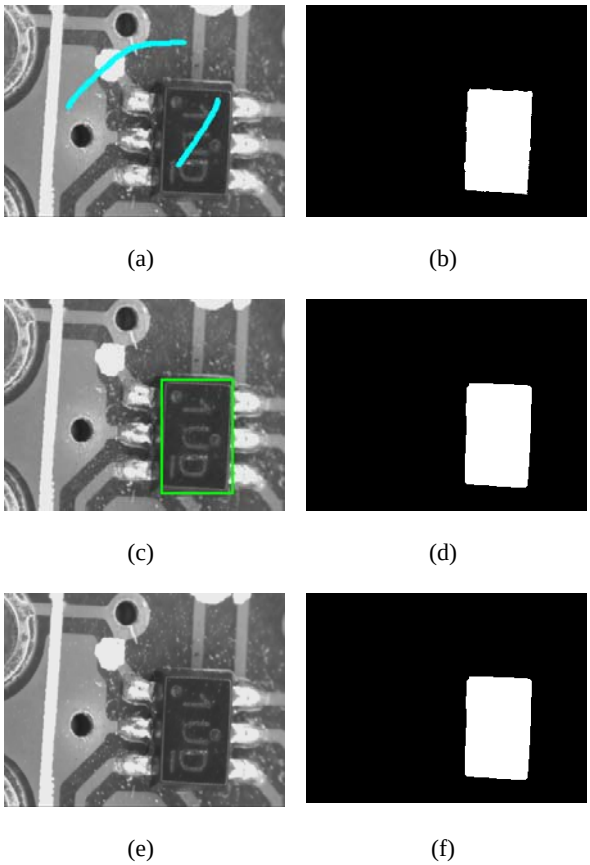

(a) (b)

(c) (d)

(e) (f)

Fig. 6. Segmentation results comparison of user intervention method and A-GrabCut method: (a) manual mark of watershed method; (b) segmentation result of watershed method; (c) manual mark of original GrabCut method; (d) segmentation result of original GrabCut method; (e) manual mark of A-GrabCut method: no mark; (f) segmentation result of A-GrabCut method.

3.2. Comparison with Binary Segmentation

As GrabCut method is popular foreground and background method, it can also be viewed as a binary classification problem. So in the second experiment,

we evaluated the performance of A-GrabCut method and a typical adaptive threshold binary segmentation method [24].

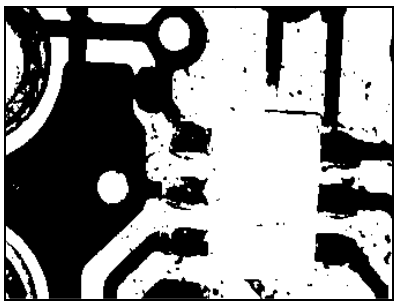

Fig. 7. Segmented result of adaptive threshold binary method.

Fig. 7 illustrates the image segmentation result by using threshold method. It can be seen that the segmentation result of A-GrabCut is much better than that of the threshold method. The threshold method computes mean and variance of pixel value and can generate a balance gray to image segmentation. As shown in Fig. 7. Though the foreground welded component has been segmented, the similar grayscale pixels are considered as homogeneous region, such as holes and some region of PCB. And most objects segmented by threshold method are with noises or incomplete edges. It is hard to satisfy the segmentation requirement.

So in brief, the proposed A-GrabCut method is much better than the naive binary classification method for image segmentation.

4. Conclusions

Due to real PCB scenery is complex and common image segmentation method cannot segmented automatically and efficiently welded components. In this paper, an automatic PCB welding component segmentation method based on GrabCut technique is proposed. The advantages of proposed A-GrabCut method include:

1) It exploits the character of welded components locating at disparity foreground region. The feature is not dependent on image intensive, shape, texture and other prior knowledge.

2) Welded component can be extracted correctly without any user intervention.

3) The proposed method is automatic, instead of processing certain region with user intervention.

In addition to these advantages, the proposed method has its limitation:

1) The trimap T of GrabCut method is dependent on the result of matching disparity map.

2) The color of mask region and non-mask region of original image cannot too similar.

References

[1]. Benedek C., Krammer O., Janóczki M., *et al.*, Solder paste scooping detection by multilevel visual inspection of printed circuit boards, *IEEE Transactions on Industrial Electronics*, Vol. 60, No. 6, 2013, pp. 2318-2331.

[2]. Aghamohammadi A., Ang M. C., Prabuwono A. S., *et al.*, Enhancing an automated inspection system on printed circuit boards using affine-SIFT and TRIZ techniques, *Advances in Visual Informatics*, 2013, pp. 128-137.

[3]. Cheng H. D., Jiang X. H., Sun Y., et al., Color image segmentation: advances and prospects, *Pattern Recognition*, Vol. 34, No. 12, 2001, pp. 2259-2281.

[4]. Estrada F. J., Jepson A. D., Benchmarking image segmentation algorithms, *International Journal of Computer Vision*, Vol. 85, No. 2, 2009, pp. 167-181.

[5]. Horng M. H., Multilevel thresholding selection based on the artificial bee colony algorithm for image segmentation, *Expert Systems with Applications*, Vol. 38, No. 11, 2011, pp. 13785-13791.

[6]. Garcia Ugarriza L, Saber E., Vantaram S. R., *et al.*, Automatic image segmentation by dynamic region growth and multiresolution merging, *IEEE Transactions on Image Processing*, Vol. 18, No. 10, 2009, pp. 2275-2288.

[7]. Wang H., Oliensis J., Generalizing edge detection to contour detection for image segmentation, *Computer Vision and Image Understanding*, Vol. 114, No. 7, 2010, pp. 731-744.

[8]. Yu Z., Au O. C., Zou R., *et al.*, An adaptive unsupervised approach toward pixel clustering and color image segmentation, *Pattern Recognition*, Vol. 43, No. 5, 2010, pp. 1889-1906.

[9]. Li Z., Wu X. M., Chang S. F., Segmentation using superpixels: A bipartite graph partitioning approach, *Computer Vision and Pattern Recognition*, 2012, pp. 789-796.

[10]. Boykov Y. Y., Jolly M. P., Interactive graph cuts for optimal boundary & region segmentation of objects in N-D images, in *Proceedings of the International Conference on Computer Vision*, Vol. 1, 2001, pp. 105-112.

[11]. Siang Tan K., Mat Isa N. A., Color image segmentation using histogram thresholding-Fuzzy C-means hybrid approach, *Pattern Recognition*, Vol. 44, No. 1, 2011, pp. 1-15.

[12]. Hammouche K., Diaf M., Siarry P., A multilevel automatic thresholding method based on a genetic algorithm for a fast image segmentation, *Computer Vision and Image Understanding*, Vol. 109, No. 2, 2008, pp. 163-175.

[13]. Ye J., Xu G., Geometric flow approach for region-based image segmentation, *IEEE Transactions on Image Processing*, Vol. 21, 12, 2012, pp. 4735-4745.

[14]. Arbelaez P., Maire M., Fowlkes C., *et al.*, Contour detection and hierarchical image segmentation, *IEEE Transactions on Pattern Analysis and Machine Intelligence*, Vol. 33, No. 5, 2011, pp. 898-916.

[15]. Wang Z., Song Q., Soh Y. C., *et al.*, An adaptive spatial information-theoretic fuzzy clustering algorithm for image segmentation, *Computer Vision and Image Understanding*, Vol. 117, No. 10, 2013, pp. 1412-1420.

[16]. Yang J., Gan Z., Gui X., *et al.*, 3-D Geometry Enhanced Superpixels for RGB-D Data, *Advances in*

Multimedia Information Processing – PCM, 2013, pp. 35-46.
[17]. Rother C., Kolmogorov V., Blake A., GrabCut: Interactive foreground extraction using iterated graph cuts, *ACM Transactions on Graphics*, Vol. 23, No. 3, 2004, pp. 309-314.
[18]. Peng B., Zhang L., Zhang D., *et al*., Image segmentation by iterated region merging with localized graph cuts, *Pattern Recognition*, Vol. 44, No. 10, 2011, pp. 2527-2538.
[19]. Fusiello A., Irsara L., Quasi-Euclidean epipolar rectification of uncalibrated images, *Machine Vision and Applications*, Vol. 22, No. 4, 2011, pp. 663-670.
[20]. Yang Q., A non-local cost aggregation method for stereo matching, in *Proceedings of the Conference on Computer Vision and Pattern Recognition*, 2012, pp. 1402-1409.
[21]. Yoon K. J., Kweon I. S., Adaptive support-weight approach for correspondence search, *IEEE Transactions on Pattern Analysis and Machine Intelligence*, Vol. 28, No. 4, 2006, pp. 650-656.
[22]. Boykov Y., Kolmogorov V., An experimental comparison of mincut/max-flow algorithms for energy minimization in vision, *IEEE Transactions on Pattern Analysis and Machine Intelligence*, Vol. 26, No. 9, 2004, pp. 1124-1137.
[23]. Vachier C., Meyer F., The viscous watershed transform, *Journal of Mathematical Imaging and Vision*, Vol. 22, No. 2-3, 2005, pp. 251-267.
[24]. Otsu N., A threshold selection method from gray-level histograms, *IEEE Transactions on Systems, Man, and Cybernetics*, Vol. 9, No. 1, 1979, pp. 62-66.